

1-1-2026

Oil Palm (*Elaeis Guineensis*) Leaf Extract-Mediated Green Synthesis of TiO₂ Nanoparticles and Their Optical Characteristics

Nofrijon Sofyan

Advanced Materials Research Center, Faculty of Engineering, Universitas Indonesia, Depok 16424, Indonesia AND Department of Metallurgical and Materials Engineering, Faculty of Engineering, Universitas Indonesia, Depok 16424, Indonesia, nofrijon.sofyan@ui.ac.id

Andriayani

Department of Chemistry, Faculty of Mathematics and Natural Sciences, University of Sumatera Utara, Medan 20155, Indonesia, andriayani@usu.ac.id

Yetria Rilda

Department of Chemistry, Faculty of Mathematics and Natural Sciences, Andalas University, Padang, 25163, Indonesia, yetriarilda@sci.unand.ac.id

Fiona Angellinnov

Department of Metallurgical and Materials Engineering, Faculty of Engineering, Universitas Indonesia, Depok 16424, Indonesia, fiona.angellinnov31@ui.ac.id

Mouna M'rad

Department Physique, Université Paris-Saclay, Bâtiment Bréguet, 91190, France, mradmouna@outlook.fr

Follow this and additional works at: <https://bsj.uobaghdad.edu.iq/home>

See next page for additional authors

How to Cite this Article

Sofyan, Nofrijon; Andriayani; Rilda, Yetria; Angellinnov, Fiona; M'rad, Mouna; Muhammad; Ridhova, Aga; Yuwono, Akhmad Herman; and Dhaneswara, Donanta (2026) "Oil Palm (*Elaeis Guineensis*) Leaf Extract-Mediated Green Synthesis of TiO₂ Nanoparticles and Their Optical Characteristics," *Baghdad Science Journal*: Vol. 23: Iss. 1, Article 6.

DOI: <https://doi.org/10.21123/2411-7986.5144>

This Special Issue Article is brought to you for free and open access by Baghdad Science Journal. It has been accepted for inclusion in Baghdad Science Journal by an authorized editor of Baghdad Science Journal.

Oil Palm (*Elaeis Guineensis*) Leaf Extract-Mediated Green Synthesis of TiO₂ Nanoparticles and Their Optical Characteristics

Authors

Nofrijon Sofyan, Andriayani, Yetria Rilda, Fiona Angellinnov, Mouna M'rad, Muhammad, Aga Ridhova, Akhmad Herman Yuwono, and Donanta Dhaneswara



SPECIAL ISSUE ARTICLE

Oil Palm (*Elaeis Guineensis*) Leaf Extract-Mediated Green Synthesis of TiO₂ Nanoparticles and Their Optical Characteristics

Nofrijon Sofyan^{1,2,*}, Andriyani³, Yetria Rilda⁴, Fiona Angellinnov², Mouna M'rad⁵, Muhammad², Aga Ridhova⁶, Akhmad Herman Yuwono^{1,2}, Donanta Dhaneswara^{1,2}

¹ Advanced Materials Research Center, Faculty of Engineering, Universitas Indonesia, Depok 16424, Indonesia

² Department of Metallurgical and Materials Engineering, Faculty of Engineering, Universitas Indonesia, Depok 16424, Indonesia

³ Department of Chemistry, Faculty of Mathematics and Natural Sciences, University of Sumatera Utara, Medan 20155, Indonesia

⁴ Department of Chemistry, Faculty of Mathematics and Natural Sciences, Andalas University, Padang, 25163, Indonesia

⁵ Department Physique, Université Paris-Saclay, Bâtiment Bréguet, 91190, France

⁶ Research Center for Metallurgy, National Research and Innovation Agency, Tangerang Selatan, Banten 15314, Indonesia

ABSTRACT

This work aims to explore the characteristics of TiO₂ NPs green-synthesized via an environmentally friendly method using oil palm (*Elaeis guineensis*) leaf extract as a green medium and capping agent by utilizing titanium tetra isopropoxide (TTIP) as precursor. The oil palm leaves were extracted with different solvent concentration variations. The natural extract was characterized using liquid chromatography-mass spectroscopy (LC-MS) and infrared spectroscopy for active chemical contents and functional groups. The obtained TiO₂ NPs were also characterized using infrared spectroscopy (FTIR) for the functional groups, ultraviolet spectroscopy (UV-DRS) for the optical characteristics, and X-ray diffraction (XRD) for the phase formation and crystallographic properties. More sophisticated equipment of field emission scanning electron microscopy equipped with energy dispersive X-ray spectroscopy (FESEM/EDX) and Raman spectroscopy were employed to reveal the characteristics of the obtained TiO₂ NPs. The results from X-ray diffraction showed that the obtained TiO₂ NPs are in pure anatase crystal structure. There is also a trend that the bandgap energy of TiO₂ NPs reduces with the use of oil palm leaves extract as a green medium. It is confirmed that the green medium affects the optical characteristics of the synthesized TiO₂ NPs by reducing the bandgap energy from 3.2 eV for commercial and the one synthesized using ethanol only to 3.12 eV by using the green medium of oil palm leaves extract. These findings will provide insight for more novel, environmentally friendly nanomaterials synthesis methods.

Keywords: Green synthesis, Nanoparticles, Natural plant extract, Oil palm, Titanium dioxide

Introduction

Titanium dioxide is an inorganic compound derived from titanium with the chemical formula TiO₂. It can be found naturally in ilmenite, rutile, and anatase. This material is widely used for its brightness and various applications, including cosmetics, paints,

foods, air purification, and bacterial degradation.¹ For a specific application, such as in nanotechnology, TiO₂ can be synthesized via many routes. Several routes are available to synthesize TiO₂ nanoparticles, including chemical² and physical methods.³ The main problem in almost all these chemical or

Received 28 February 2025; revised 9 August 2025; accepted 16 August 2025.
Available online 1 January 2026

* Corresponding author.

E-mail addresses: nofrijon.sofyan@ui.ac.id (N. Sofyan), andriyani@usu.ac.id (Andriyani), yetriarilda@sci.unand.ac.id (Y. Rilda), fiona.angellinnov31@ui.ac.id (F. Angellinnov), mradmouna@outlook.fr (M. M'rad), muhammad93@ui.ac.id (Muhammad), aga.ridhova@brin.go.id (A. Ridhova), ahyuwono@eng.ui.ac.id (A. H. Yuwono), donanta.dhaneswara@ui.ac.id (D. Dhaneswara).

International Conference on Discoveries in Applied Sciences and Applied Technology (DASAT2025)

<https://doi.org/10.21123/2411-7986.5144>

2411-7986/© 2026 The Author(s). Published by College of Science for Women, University of Baghdad. This is an open-access article distributed under the terms of the Creative Commons Attribution 4.0 International License, which permits unrestricted use, distribution, and reproduction in any medium, provided the original work is properly cited.

physical processes is the less eco-friendly approach, and thus they may impose risks to the environment.^{4,5} Because of that, an environmentally friendly method to synthesize TiO₂ NPs by utilizing natural resources in the form of extracts from plant parts^{6,7} has attracted special attention due to its simple protocol, cost-effectiveness, and sustainability.⁸ The process involves simple steps in selecting suitable plant parts, solvent, and non-toxic elements during production.⁹ The utilization of these natural resources has many advantages, such as energy efficiency, product selectivity, and safety for human health and the environment.¹⁰

Several plant extracts have been used as media for the green synthesis of metal oxide nanoparticles, with a broad range of applications. Septingrum et al. used mangosteen pericarp extract as a medium in green-synthesizing Ag/TiO₂ nanocomposites for pollutant degradation.⁶ Hussain et al. have explored the use of *Morus nigra* leaf extract as a medium in green-synthesizing TiO₂ nanoparticles with biological potential.¹¹ Rajendhiran et al. have analyzed the characteristics of TiO₂ nanoparticles green-synthesized using *Terminalia catappa* and *Carissa carandas* fruit extracts.¹² Sofyan et al. used *Terminalia catappa* fruit extract as a medium for green-synthesizing TiO₂ nanoparticles and applied the resulting nanoparticles as a semiconductor layer in a dye-sensitized solar cell.⁸ Patil and his coworker used *Bixa orellana* seed extract as a green medium to synthesize silver nanoparticles for pharmacological applications,¹³ while Maurya et al. used it as a medium to synthesize green TiO₂ nanoparticles for solar cell applications.¹⁴ Olewi et al. have explored the use of orange peel as a green medium for synthesizing TiO₂ nanoparticles, comparing it with the conventional sol-gel method.¹⁵ Recently, Sofyan et al. have also investigated the properties of TiO₂ nanoparticles green-synthesized with *Uncaria gambir* extract for dye-sensitized solar cell applications.¹⁶

Oil palm (*Elaeis guineensis*) is a species of palm tree that is widely cultivated for its oil-rich fruits. It is well known that its leaves are rich in catechins and polyphenols.^{17,18} Several investigators have used oil palm leaves as free radical scavengers,¹⁹ antibacterials,²⁰ and adsorbers for pollution.²¹ However, in the plantation, the leaves are mostly discarded and left to decompose between the oil palm trunks.²² Considering the active contents of the oil palm leaves, there is a possibility that this extract from oil palm leaves could be useful as a medium in an eco-friendly synthesis of TiO₂ NPs. To the best of the authors' knowledge, no literature has been published on using oil palm leaves as a medium in the green synthesis of TiO₂ NPs. In this study, oil palm leaves were

extracted using various solvents and concentrations. The extract was then utilized as a medium for the green synthesis of TiO₂ NPs. The primary objective of this work is to investigate the characteristics of TiO₂ NPs green-synthesized using oil palm leaf extract, which can later be employed in photocatalysis and/or energy harvesting applications.

Materials and methods

Materials

The chemicals include ethanol (Merck), acetylacetone (C₅H₈O₂, Sigma Aldrich), commercial TiO₂ (Merck), polyvinylidene fluoride (PVDF, Merck), N-Methyl-2-pyrrolidone (NMP, Merck), commercial dye N719 (C₅₈H₈₆O₈N₈S₂Ru, Solaronix), platinum paste (Platisol, Solaronix), and electrolyte solution (Iodolyte Z-50, Solaronix). The precursor for the synthesis of TiO₂ was titanium tetra isopropoxide (TTIP, Ti{OCH(CH₃)₂}₄, Sigma Aldrich). All chemicals are reagent grade and were used without further treatment.

Oil palm leaf extract preparation

The oil palm leaf extract was prepared following the work of others¹⁷ with slight modifications, as explained below: Oil palm leaves obtained from a farmer in Pangkalan, West Sumatra, were cleaned under running tap water and allowed to dry before being chopped with a sharp knife. Four different extract variations were prepared using ethanol with 0, 10, 30, and 50% acetylacetone. In this work, acetylacetone was used as a chelating agent to control the growth, stability, and crystallinity of TiO₂ nanoparticles.²³ For each variation, 20 g of chopped oil palm leaf was blended in 100 mL of solvent using a household blender for five minutes. Further, the mixture was filtered to separate the insoluble residue from the solvent, and extracts from the oil palm leaf with varying solvent concentrations were obtained and stored in a dark bottle. The oil palm leaf extract was analyzed for its chemical composition and functional groups using liquid chromatography-mass spectrometry (LC-MS; ACQUITY UPLC® H-Class System-Xevo G2-S QToF, Waters) and Fourier transform infrared spectroscopy (FTIR; PerkinElmer ATR Spectrum One).

Green synthesis of TiO₂ nanoparticles

The environmentally friendly synthesis of titanium dioxide in the oil palm extract medium followed the sol-gel method²⁴ with slight modification. The

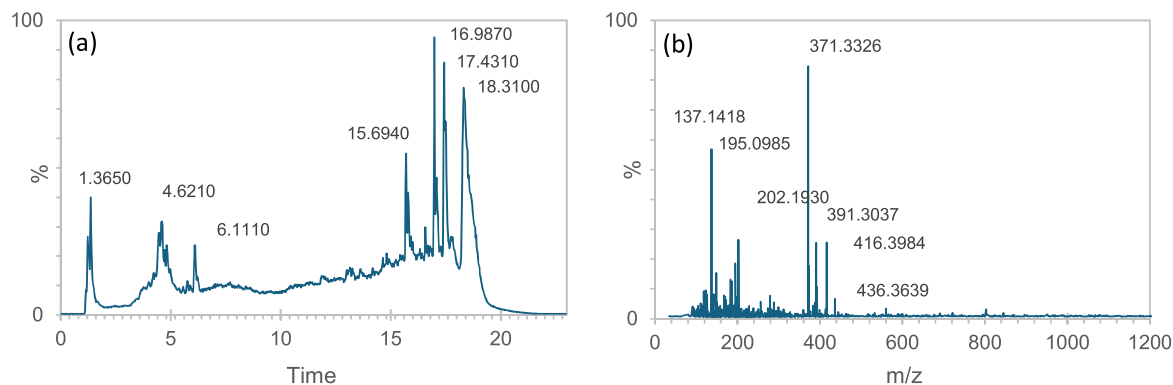


Fig. 1. Oil palm leaf extract (a) chromatogram and (b) spectrum obtained using LC-MS spectroscopy.

procedure is explained as follows. Five beaker glasses were prepared, and 10 mL of titanium tetra isopropoxide (TTIP, $\text{Ti}\{\text{OCH}(\text{CH}_3)_2\}_4$, Sigma Aldrich) was emptied into each beaker glass. Ten mL of ethanol was added dropwise to the first beaker glass (labelled as Eth), and ten mL of oil palm extract from various solvents explained in the previous section was added dropwise to the rest of the beaker glasses and labelled as P0, P10, P30, and P50, respectively. The mixture was agitated with a magnetic stirrer for 3 hours, then left overnight and filtered to obtain a wet gel. The gel was dried at 100 °C for 1 hour and calcined at 450 °C for 2 hours to obtain white powders of TiO_2 NPs. The obtained products were examined using FTIR, ultraviolet-visible spectroscopy (UV-Vis, Shimadzu UV2450), X-ray diffraction (XRD, AERIS Malvern PANalytical), Raman spectroscopy (HORIBA iHR320), and field emission scanning electron microscopy coupled with energy dispersive X-ray spectroscopy (FESEM/EDX, FEI Inspect F50). For characterization using UV-Vis and XRD, the number of specimens was triplicate for statistical analysis, employing one-way analysis of variance (ANOVA) in MatLAB®.

Results and discussion

Active contents and functional groups

We obtained the chromatogram and mass spectrum of the active components in oil palm leaf extract using LC-MS. As can be seen from the chromatogram and spectrum given in Fig. 1a and 1b, respectively, oil palm leaf extract is detected to contain several active chemical compounds, most of which are dominated by tolylsulfonic acid at retention times 3.6–4.6, propenoic acid at retention times 5.6–6.1, and dicyclohexyl ethyl phosphate at retention times 14.4–15.7, as well as other unidentified active chemical components at higher retention times. These

active compounds are expected to play an essential role in the green synthesis of TiO_2 nanoparticles.

To confirm the active compounds identified by LC-MS, the oil palm leaf extract was further analyzed by infrared spectroscopy. This infrared absorption can be further used to determine the functional groups present in the molecule. The functional group spectrum of the oil palm leaf extract obtained using infrared spectroscopy is given in Fig. 2a, whereas the infrared spectra of commercial TiO_2 NPs, TiO_2 NPs synthesized using ethanol only, and TiO_2 NPs synthesized via the green method using oil palm leaf extract are given in Fig. 2b. The infrared spectrum of oil palm leaf extract shows several absorption bands. In general, as can be seen from the figure, a broad signal is detected at 3000–3600 cm^{-1} from the O-H group as an indication of a phenol compound. The presence of the C=C group with the ring of aromatic compound is detected at 1570.12 cm^{-1} ; the alkane compound with C-H stretching is detected at 1417.74 cm^{-1} ; the type of alkene compound with C=C bending is detected at 751.31–872.83 cm^{-1} ; whereas the typical alcohol compound with medium weak intensity of C-O stretching is detected at 1069.57–1181.45 cm^{-1} . The absorption peaks at the regions 3366 cm^{-1} , 1650 cm^{-1} , and 679 cm^{-1} are expected from the characteristics of flavonoids²⁵ and as an indication of the presence of quercetin and related compounds known as flavonoid compounds. The yellow colors in the oil palm leaf extract are expected to be due to hydroxy and methoxy derivatives of flavones and isoflavones²⁶ and are believed to influence the crystal growth of TiO_2 NPs during the green synthesis.²⁷

To observe how oil palm leaf extract affects the characteristics of TiO_2 NPs after green synthesis, researchers collected the spectra of TiO_2 NPs and those from commercial TiO_2 , which are provided in Fig. 2b. For commercial TiO_2 NPs, weak stretching vibrations of hydrogen-bonded water molecules, bending vibrations of the C=C group, and the Ti-O-Ti bridging

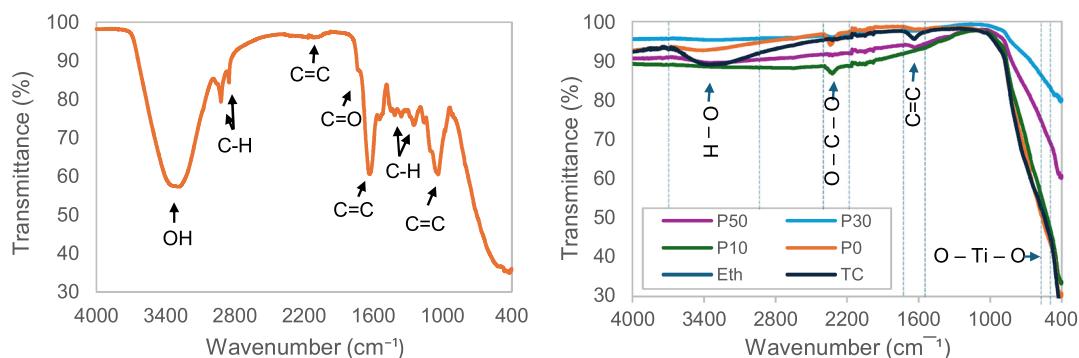


Fig. 2. Infrared spectra of (a) oil palm leaf extract and (b) TiO₂ NPs: commercial (TC), synthesized using ethanol (Eth), and green-synthesized using oil palm leaf extract (P0).

stretching mode are detected at around 3370, 1630, and 650 cm⁻¹, respectively.²⁸ The presence of OH groups is expected due to the interaction of TiO₂ NPs with environmental moisture.²⁹ The same characteristics were also found in the spectrum of TiO₂ obtained from the synthesis using pure ethanol (Eth) and the green synthesis using extracts from oil palm leaves. An additional weak absorption at 2326 cm⁻¹ is also observed, possibly due to O-C-O linear vibrations, as reported in another study.⁸ The presence of a certain amount of carbon in TiO₂ NPs may affect morphology, crystallinity, and bandgap energy as reported by others.^{30,31}

Optical characteristics

UV-Vis spectroscopy is primarily used to measure a material's light absorption and determine its optical properties, such as the band gap energy. In this work, the optical characteristics of commercial TiO₂ NPs and those obtained from the synthesis were analyzed using UV-Vis DRS. The obtained reflectance spectra (not shown) were further analyzed to determine their bandgap energies using the Kubelka–Munk relation.³² Firstly, the data was fitted in the Tauc plot $(F(R_{\infty}) \cdot hc/\lambda)^{1/2}$ vs hc/λ , assuming the sample has an indirect allowed electron transition.³³ The results from this fitting are illustrated in Fig. 3. By extrapolating the linear part of the Tauc plot to the intersection point of the x-axis, an estimated value of the band gap energy for each TiO₂ NPs was obtained to be 3.20(0.00) eV, 3.20(0.02) eV, and 3.12(0.08) eV for commercial, synthesized using ethanol, and green-synthesized using oil palm leaf extract, respectively. Based on the obtained bandgap energies, the bandgap decreases when a green medium is used. This decrease is expected due to the active chemical contents in the oil palm extract during the synthesis.

For the optical characteristics of TiO₂ NPs green-synthesized with the addition of acetylacetone as a

chelating agent, as shown in Fig. 3d, 3e and 3f, the bandgap energy decreases with increasing acetylacetone concentration, i.e., 3.08(0.09) eV, 3.00(0.07) eV, and 2.99(0.08) eV for 10%, 30%, and 50% acetylacetone concentrations, respectively. The values in parentheses indicate the standard error. Statistical analysis shows a significant difference in bandgap energy (p -value = 0.01), which is smaller than the alpha-value of 0.05. It is believed that the decrease in bandgap energy is due to the use of a chelating agent during the green synthesis of TiO₂ NPs. In terms of applications, reduced bandgap energy will play a crucial role in photocatalysis and light-harvesting applications, such as pollutant degradation and dye-sensitized solar cells. A lower bandgap allows materials to absorb a broader spectrum of light, particularly in the visible range, thereby significantly improving the efficiency of converting solar energy into chemical or electrical energy.³⁴

Surface morphology and chemical composition

The surface morphology and chemical composition of the obtained TiO₂ NPs were examined using FESEM coupled with EDX. The results, in terms of chemical composition and surface morphology, of commercial TiO₂ NPs synthesized using ethanol only and green-synthesized using oil palm extract are presented in Figs. 4 and 5, respectively. The EDX spectra show that the main peaks of titanium and oxygen are clearly visible. This means that TiO₂ is present and that the green synthesis process worked. In addition, the weight fraction of titanium (62–67%) and oxygen (32–38%) confirms the successful green synthesis of TiO₂ NPs using oil palm leaf extract as a medium and capping agent.^{35,36} Before FESEM characterization, the TiO₂ NPs were coated using Au/Pd³⁷ to increase their conductivity, which is confirmed as unlabelled peaks around 2 keV in the EDX spectra.³⁸ The presence of the carbon element, as detected using FTIR, cannot

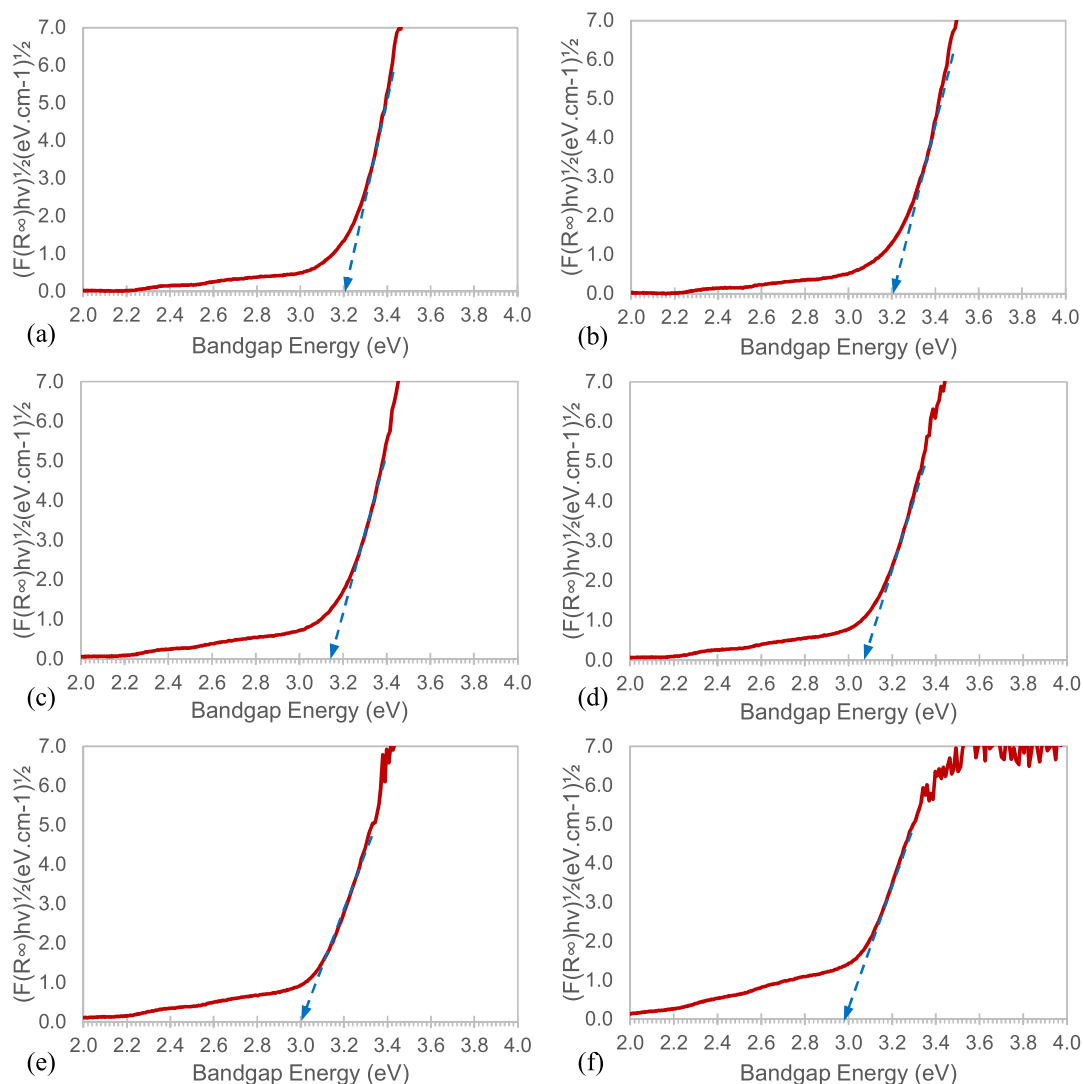


Fig. 3. Tauc plots for bandgap energy determination of (a) commercial TiO_2 , (b) TiO_2 synthesized using ethanol only, (c) TiO_2 synthesized using oil palm leaf extract only, (d) TiO_2 synthesized using oil palm leaf extract with 10%, (e) 30%, and (f) 50% acetylacetone.

be identified in the EDX spectrum, probably due to the limitations of the EDX technique.

As shown in Fig. 5, the electron image of commercial TiO_2 (TC) reveals homogeneous sphere-like particles but tends to be agglomerated. Measurement using ImageJ® revealed an average particle size of 190 nm. For the synthesis using ethanol only (Eth), the round morphology is maintained, but the tendency to agglomerate makes the particles appear larger than those of the commercial one, with an average particle size of 345 nm. With the addition of oil palm leaf extract as a medium in the green synthesis, as shown in Fig. 4, the round-shaped particles remain, with a particle size smaller than that of TiO_2 synthesized using ethanol only and resembling that of commercial TiO_2 with an average particle size of 200 nm. Since the medium is the only difference in the

synthesis methods, it is confirmed that oil palm leaf extract affects the particle growth of TiO_2 NPs during the green synthesis. For the samples with the addition of acetylacetone as a chelating agent, as shown in Fig. 5d, 5e and 5f, the electron images indicate that the particle size tends to agglomerate and form large particles at low (10%) and high (50%) acetylacetone concentrations with an average particle size of 486 nm and 625 nm, respectively. The tendency to agglomerate appears low at a 30% acetylacetone concentration, with an average particle size of 430 nm.

Crystallographic properties

X-ray diffraction is a powerful method for determining a material's crystallographic properties. In this

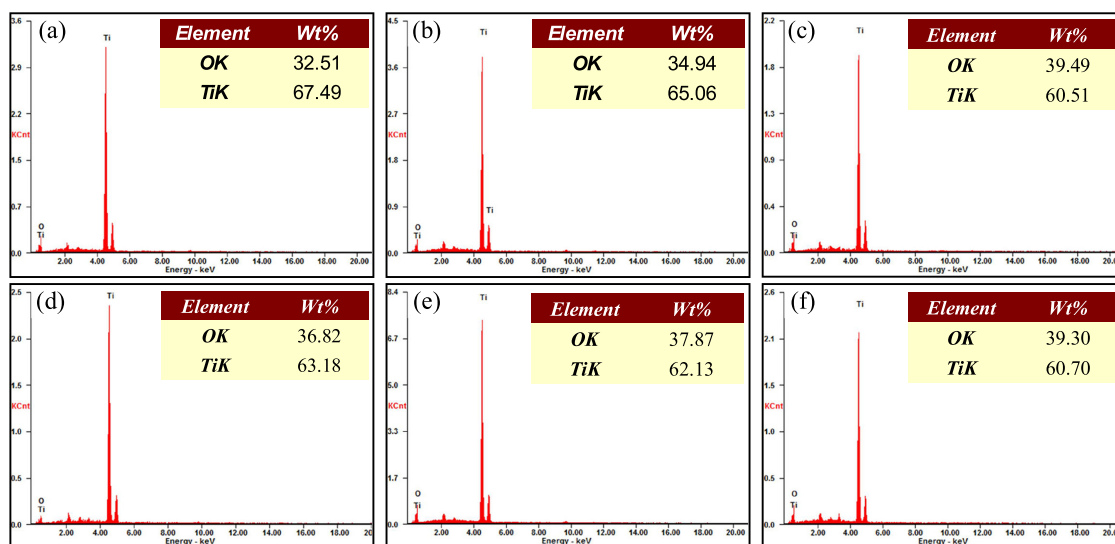


Fig. 4. Energy dispersive X-ray spectra of (a) commercial TiO₂ NPs, (b) TiO₂ synthesized using ethanol only, and TiO₂ NPs green-synthesized using oil palm leaf extract with (c) 0%, (d) 10%, (e) 30%, and (f) 50% acetylacetone. Elemental compositions are given in the inset table.

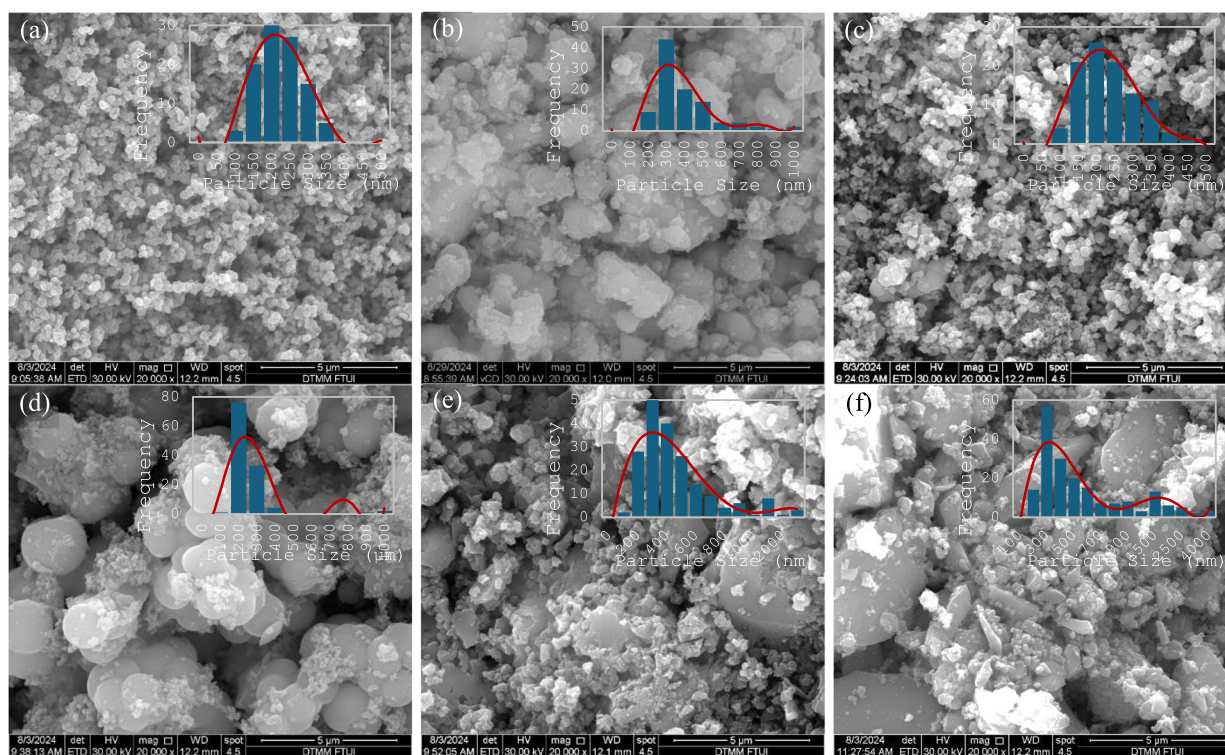


Fig. 5. Secondary electron images of (a) commercial TiO₂, (b) TiO₂ NPs synthesized using ethanol only, (c) TiO₂ NPs green-synthesized using oil palm leaf extract with acetylacetone concentration variations (c) 0%, (d) 10%, (e) 30%, and (f) 50%. The inset graph is the particle size distribution.

work, powder X-ray diffraction was used to analyze the crystallographic properties of TiO₂ NPs synthesized via green methods. As comparisons, commercial TiO₂ NPs and TiO₂ NPs synthesized using ethanol only were also examined. The results are provided

in Fig. 6. The diffractogram of commercial TiO₂ NPs shows very sharp peaks around 2θ 25.0°, 36.6°, 37.5°, 38.3°, 47.7°, 53.6°, 54.8°, 62.4°, 68.5°, 70.2°, and 74.8°, indicating the presence of (101), (103), (004), (112), (020), (105), (211), (204), (116), (220), and

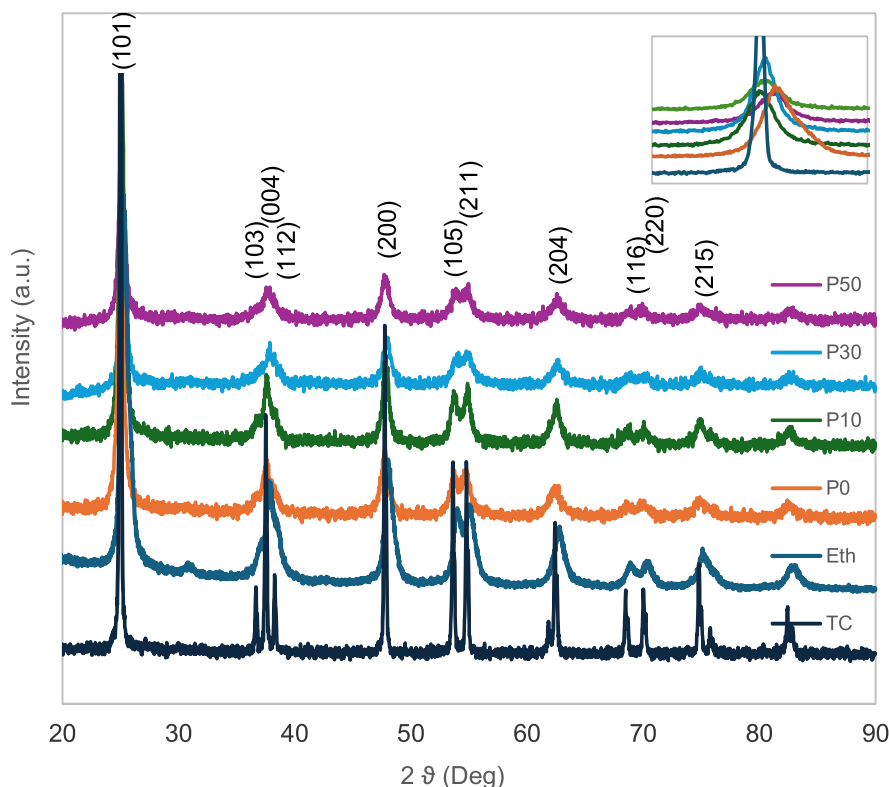


Fig. 6. X-ray diffractograms of TiO_2 NPs (TC), synthesized using ethanol only (Eth), and green-synthesized using oil palm leaf extract with 0% (P0), 10% (P10), 30% (P30), and 50% (P50) acetylacetone. The inset shows a peak shift.

(215) planes, respectively. No other impurities were detected. The analysis indicated that these peaks belong to the anatase phase (ICSD 98-000-9853). At the same time, the diffractograms of the obtained TiO_2 NPs also reveal the same prominent peaks as the commercial TiO_2 NPs (ICSD 98-015-4604), also with no other phase detected except for the one synthesized using ethanol only at around 31.6° due to the presence of the brookite phase (ICSD 98-015-4605).^{8,39} These findings agree with the results obtained by others.⁴⁰

As shown in the diffractogram, the obtained TiO_2 NPs exhibit high crystallinity, as indicated by sharp, intense peaks. No new peaks indicative of phase formation were detected in the green medium with the green extract. It can be confirmed that using a green medium has not affected crystal structure formation during the green synthesis. However, as can be inspected in the plane (101), a slight shift is observed in all peaks of the synthesized TiO_2 NPs to the higher angle as compared to that of commercial TiO_2 NPs. This shift is expected due to crystallite size and lattice strain,⁴¹ which affect the Bragg peak and shift the peak angle accordingly. This shift was also observed in our previous work.⁸ To further deepen our understanding of the effect of green medium solvent variations on the crystallographic properties of TiO_2

NPs, Rietveld analysis was performed using Highscore Plus^{42,43} on all TiO_2 NPs diffractograms. The results, summarized after Rietveld refinement, are presented in Table 1.

The refinement indicated that there is no effect of the green medium or the chelating agent on the lattice parameters and, consequently, on the unit cells. For the crystallite size, there is a tendency for it to decrease with the use of palm leaf extract compared with commercial TiO_2 and with ethanol-only synthesis. With the addition of acetylacetone, the crystallite size increases at low concentration and then decreases again with the increase of acetylacetone concentration. One-way analysis of variance shows that there is indeed a significant difference in crystallite size (p -value = 0.0267), which is smaller than the alpha-value of 0.05.

To compare with the results obtained in this work, Table 2 presents the media used for the green synthesis of TiO_2 NPs and their key parameters across different plant sources.

Raman spectroscopy

Raman spectroscopy is a powerful technique to identify chemical structures and compositions by analyzing how light interacts with molecular bonds. In

Table 1. Lattice parameters of TiO₂ NPs from the green synthesis and the commercial one.

| Sample | Lattice parameter | | | Goodness of fit (χ^2) | Crystallite size (nm) |
|--------|-------------------|-----------|--------------------|------------------------------|-----------------------|
| | a (Å) | c (Å) | V (Å) ³ | | |
| TC | 3.7806(1) | 9.5017(3) | 135.8053 | 1.0533 | 96.4616(0.00) |
| Eth | 3.7858(5) | 9.4990(2) | 136.1514 | 1.9600 | 10.7745(0.75) |
| P0 | 3.7864(5) | 9.4990(2) | 136.1845 | 1.0000 | 9.5606(0.07) |
| P10 | 3.7857(5) | 9.5069(1) | 136.2284 | 1.2763 | 11.5779(0.01) |
| P30 | 3.7920(1) | 9.5000(3) | 136.6238 | 1.9209 | 9.8167(0.15) |
| P50 | 3.7883(9) | 9.4880(3) | 136.1611 | 1.4748 | 9.2924(0.38) |

Table 2. A comparative table of key parameters from the green synthesis of TiO₂ NPs across plant sources.

| Medium | Variation | Phase | Bandgap (eV) | Crystallite Size nm) |
|---|-------------------------------------|------------------|--------------|----------------------|
| Mangosteen pericarp (MP) ⁶ | TiO ₂ P25 | Anatase/rutile | 3.17 | - |
| | Ag/TiO ₂ 5 mM | Anatase/rutile | 3.09 | - |
| | Ag/TiO ₂ 15 mM | Anatase/rutile | 3.06 | - |
| | Ag/TiO ₂ 45 mM | Anatase/rutile | 3.00 | - |
| Tropical almond (TA) fruit ⁸ | TiO ₂ P25 | Anatase/rutile | 3.19 | 17.03 |
| | No TA | Anatase/brookite | 3.19 | 12.53 |
| | 0.6% TA | Anatase | 3.14 | 10.43 |
| | 0.8% TA | Anatase | 3.12 | 12.93 |
| | No TA + 0.0017% graphene oxide (GO) | Anatase | 3.18 | 16.30 |
| | 0.6% TA + 0.0017% GO | Anatase | 3.16 | 11.83 |
| | 0.8% TA + 0.0017% GO | Anatase | 3.16 | 9.31 |
| | No TA + 0.16% GO | Anatase | 3.16 | 18.32 |
| | 0.6% TA + 0.16% GO | Anatase | 3.15 | 13.61 |
| | 0.8% TA + 0.16% GO | Anatase | 3.15 | 11.62 |
| Tropical almond (TA) and <i>Carissa carandas</i> (CC) ¹² | 0.2% TA | Anatase | 3.28 | 21.00 |
| | 0.4% TA | Anatase | 3.26 | 17.00 |
| | 0.6% TA | Anatase | 3.24 | 12.00 |
| | 0.8% TA | Anatase | 3.21 | 8.00 |
| | 0.2% CC | Anatase | 3.30 | 20.00 |
| | 0.4% CC | Anatase | 3.28 | 19.00 |
| | 0.6% CC | Anatase | 3.26 | 15.00 |
| | 0.8% CC | Anatase | 3.24 | 10.00 |
| | No BO | Anatase/brookite | 3.20 | 13.00 |
| | With BO | Anatase | 2.90 | 9.00 |
| Orange peel (OP) ¹⁵ | No OP | Anatase/brookite | 2.85 | 30.20 |
| | With OP | Anatase | 3.25 | 24.90 |

this work, Raman spectra were used to confirm the X-ray diffraction analysis. As shown in Fig. 7a, the spectrum of commercial TiO₂ NPs shows a strong characteristic as indicated by the peaks centering at 143 cm⁻¹, 197 cm⁻¹, 396 cm⁻¹, 514 cm⁻¹, and 637 cm⁻¹. These peaks are attributed to the anatase phase.^{44,45} Hence, it is confirmed that the commercial TiO₂ NPs contains 100% anatase. The spectrum of TiO₂ NPs synthesized using ethanol only (Eth) shows the same characteristics as that of commercial TiO₂ NPs, but with the addition of a tiny peak at around 326 cm⁻¹. This little peak is due to a small brookite phase, as detected by XRD analysis mentioned in the previous section.⁴⁶ The Raman spectra of green-synthesized TiO₂ NPs follow the same trend as the commercial one and are present in a pure tetragonal anatase phase. A slight blue shift as illustrated in Fig. 7b, however, is detected as indicated by the

corresponding five characteristics with the principal peak locating around 144 cm⁻¹ followed by other peaks at 197-199 cm⁻¹, 397 cm⁻¹, 516 cm⁻¹, and 638 cm⁻¹. This blue shift is expected due to variations in crystallite size, as reported by others.⁴⁷ The characteristics obtained from these Raman spectra are consistent with the findings revealed by the X-ray diffraction analysis.

Reaction mechanism

To better understand the mechanism behind the green synthesis of TiO₂ nanoparticles (NPs) using oil palm leaf extract, we present a proposed formation mechanism that focusses on both the hydrolysis reaction alone and the hydrolysis reaction in conjunction with the green medium. As has been previously mentioned, with no green medium from the oil palm leaf

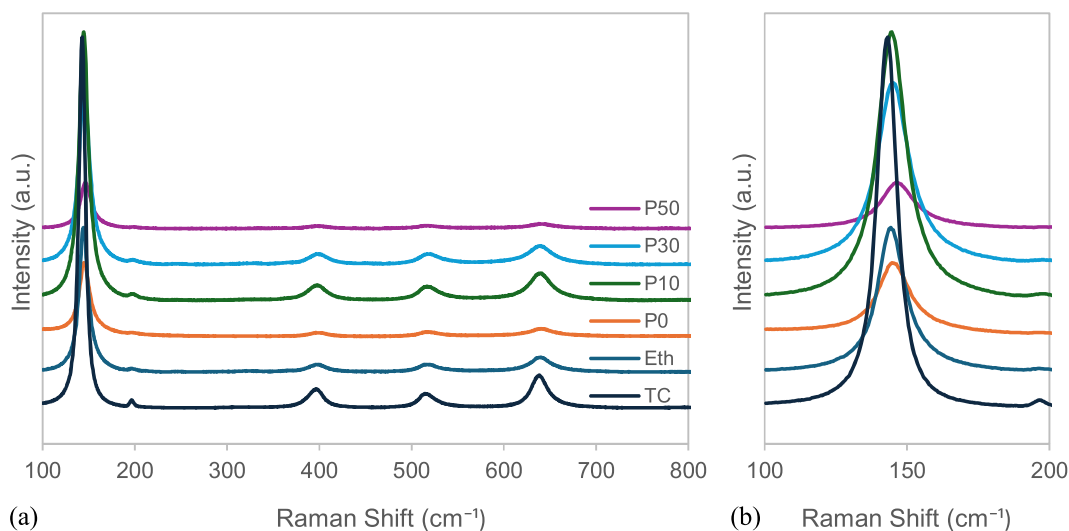
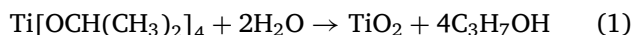


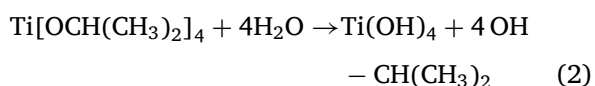
Fig. 7. (a) Superimposed Raman spectra of TiO₂ NPs (TC), synthesized using ethanol only (Eth), and green-synthesized using oil palm leaf extract with 0% (P0), 10% (P10), 30% (P30), and 50% (P50) acetylacetone at 800-100 cm⁻¹, and (b) the region zoomed at 200-100 cm⁻¹ shows the blue shift.

extract, the formation of TiO₂ is merely controlled by hydrolysis and condensation reactions represented by the following reaction:⁴⁸

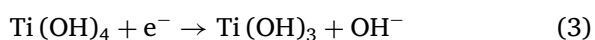


In the presence of oil palm leaves, other factors influence the growth of TiO₂ NPs during the green synthesis, i.e., the active components in the oil palm leaves. In this instant, the reduction of TTIP to TiO₂ involved several reaction steps:⁴⁹

- 1. Formation of titanium hydroxide species:



- 2. Reduction of titanium precursor:



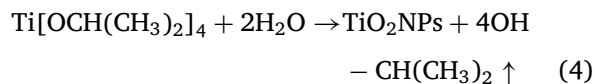
- 3. Nucleation and growth:

During nucleation and growth, reduced titanium species form nuclei and subsequently grow into TiO₂ NPs, involving a series of redox reactions that take oxygen from the surrounding environment.

- 4. Growth control and stabilization:

During the nucleation and growth process, the active compounds in the oil palm leaf extract, such as quercetin and gallic, can be adsorbed onto the surface of the forming TiO₂ NPs, which will, in turn, control and stabilize the formation of TiO₂ NPs by preventing agglomeration and providing surface modifications.

- 5. The overall formation reaction of TiO₂ NPs using the oil palm leaf extract can then be summarized as:



Conclusion

Researchers successfully carried out the environmentally friendly green synthesis of TiO₂ NPs using oil palm leaf extract as reducing and capping agents. All characterizations confirmed the successful outcome of the environmentally friendly synthesis. Although the presence of carbon was detected in the obtained TiO₂ product, it does not alter the TiO₂ NPs crystal structure. There is a tendency for the crystallite size to decrease with the use of palm leaf extract compared with commercial TiO₂ and that synthesized with ethanol only; however, the crystallite size is independent of the chelating agent concentration. The use of a green medium in the synthesis of TiO₂ NPs has also been shown to control the optical characteristics by reducing the bandgap energy, i.e., 3.2 eV for commercial TiO₂ and for TiO₂ synthesized using only ethanol, to 3.12 eV with the green medium of oil palm leaf extract. The bandgap energy of TiO₂ NPs green-synthesized in the presence of acetylacetone also reduces with an increase of acetylacetone concentration, i.e., 3.08 eV, 3.00 eV, and 2.99 eV for 10%, 30%, and 50% acetylacetone concentrations, respectively. A lower bandgap allows materials to absorb a broader spectrum of light,

particularly in the visible range. Hence, reduced bandgap energy will play an essential role in photocatalysis and light-harvesting applications, such as pollutant degradation and dye-sensitized solar cells. The future of green synthesis also aligns with the global drive for sustainable, eco-friendly technologies because green synthesis methods use naturally occurring reducing and capping agents, eliminating the need for toxic chemicals and making the process safer for both the environment and human health.

Acknowledgement

The authors acknowledge funding from Riset Kolaborasi Indonesia (RKI), managed by Universitas Indonesia, Universitas Sumatera Utara, and Universitas Andalas, as listed in the funding section.

Authors' declaration

- Conflicts of Interest: None.
- We hereby confirm that all the figures and tables in the manuscript are ours. Furthermore, any figures and images that are not ours have been included with the necessary permission for republication, which is attached to the manuscript.
- No animal studies are present in the manuscript.
- No human studies are present in the manuscript.
- Ethical Clearance: The project was approved by the local ethical committee at Universitas Indonesia, Depok 16424, Indonesia.

Authors' contribution statement

N.S.: conceptualization, formal analysis, funding acquisition, methodology, validation, writing – original draft, review, and editing. A.: data curation, funding acquisition, investigation. Y. R.: data curation, funding acquisition, investigation. F.A.: data curation, investigation, and visualization. M. M.: data curation and investigation. M.: data curation and investigation. A. R.: data curation, investigation, and visualization. A.H. Y.: writing – review and editing. D.D.: writing – review and editing.

Data availability

Data will be made available upon request.

Funding statement

Universitas Indonesia, Grant No. NKB-755/UN2.RST/HKP.05.00/2024.

Universitas Sumatera Utara, Grant No. 20/UN5.4.10.K/PPM/KP-RKI/2024.

Universitas Andalas, Grant No. 21/UN16.19/PT.01.03/RKI/2024.

References

1. Randhawa KS. Synthesis, properties, and environmental impact of hybrid pigments. *Sci World J.* 2024 Nov 01 [cited 2025 Feb 26];2024(1);2024(1). <https://doi.org/10.1155/tswj/2773950>.
2. Aboulouard A, Gultekin B, Can M, Erol M, Jouaiti A, Elhadadi B, *et al.* Dye sensitized solar cells based on titanium dioxide nanoparticles synthesized by flame spray pyrolysis and hydrothermal sol-gel methods: A comparative study on photovoltaic performances. *J Mater Res Technol.* 2020 Mar 01 [cited 2025 Feb 26];9(2):1569–1577. <https://doi.org/10.1016/j.jmrt.2019.11.083>.
3. Xu K, Chen J. High-resolution scanning probe lithography technology: a review. *Appl Nanosci.* 2020 Apr 01 [cited 2025 Feb 26];10(4):1013–1022. <https://doi.org/10.1007/s13204-019-01229-5>.
4. Naidu R, Biswas B, Willett IR, Cribb J, Singh KB, Nathanail CP, *et al.* Chemical pollution: A growing peril and potential catastrophic risk to humanity. *Environ Int.* 2021 Nov 01 [cited 2025 Feb 26];156. <https://doi.org/10.1016/j.envint.2021.106616>.
5. Lata S, Siddharth. Sustainable and eco-friendly approach for controlling industrial wastewater quality imparting succour in water-energy nexus system. *Energy Nexus.* 2021 Dec 15 [cited 2025 Feb 26];3. <https://doi.org/10.1016/j.nexus.2021.100020>.
6. Septiningrum F, Yuwono AH, Maulana FA, Nurhidayah E, Dhaneswara D, Sofyan N, *et al.* Mangosteen pericarp extract mediated synthesis of Ag/TiO₂ nanocomposite and its application on organic pollutant degradation by adsorption-photocatalytic activity. *Curr Res Green Sustain Chem.* 2024 Jan 01 [cited 2024 Dec 15];8. <https://doi.org/10.1016/j.crgsc.2023.100394>.
7. Verma V, Al-Dossari M, Singh J, Rawat M, Kordy MGM, Shaban M. A review on green synthesis of TiO₂ NPs: Synthesis and applications in photocatalysis and antimicrobial. *Polymers (Basel).* 2022 Apr 01 [cited 2025 Feb 26];14(7). <https://doi.org/10.3390/polym14071444>.
8. Sofyan N, Jamil AM, Ridhova A, Yuwono AH, Dhaneswara D, Fergus JW. Graphene oxide doping in tropical almond (*Terminalia catappa* L.) fruits extract mediated green synthesis of TiO₂ nanoparticles for improved DSSC power conversion efficiency. *Heliyon.* 2024 Apr 30 [cited 2024 Dec 15];10(8). <https://doi.org/10.1016/j.heliyon.2024.e29370>.
9. Bekele TE, Gonfa BA, Sabir FK. Use of different natural products to control growth of titanium oxide nanoparticles in green solvent emulsion, characterization, and their photocatalytic application. *Bioinorg Chem Appl.* 2021 Mar 13 [cited 2025 Feb 26];2021(1):6626313. <https://doi.org/10.1155/2021/6626313>.
10. Bordiwala R V. Green synthesis and applications of metal nanoparticles.- a review article. *Results Chem.* 2023 Feb 03 [cited 2025 Feb 26];5. <https://doi.org/10.1016/j.rechem.2023.100832>.
11. Hussain S, Nazar W, Tajammal A, Nasreen Z, Ahmad T, Ashgar A, *et al.* Green synthesis of TiO₂ nanoparticle in morus nigra leaves; characterization and biological potential. *Pol J*

- Environ Stud. 2024 Feb 12 [cited 2025 Feb 26];33(3):2707–2714. <https://doi.org/10.15244/pjoes/175060>.
12. Rajendhiran R, Deivasigamani V, Palanisamy J, Masan S, Pitchaiya S. Terminalia catappa and carissa carandas assisted synthesis of TiO₂ nanoparticles - A green synthesis approach. Mater Today: Proc. 2021 Nov 19 [cited 2024 Dec 02];452232–2238. <https://doi.org/10.1016/j.matpr.2020.10.223>.
 13. Patil SS, Nitalikar MM, khulbe P. Design, development and optimization of bixa orellana extract loaded silver nanoparticle. Adv Pharmacol Pharm. 2024 Apr [cited 2025 Feb 24];12(2):125–134. <https://doi.org/10.13189/app.2024.120205>.
 14. Maurya I C, Singh S, Senapati S, Srivastava P, and Bahadur L, “Green synthesis of TiO₂ nanoparticles using Bixa orellana seed extract and its application for solar cells,” Solar Energy, 2019 Dec 1 [cited 2025 May 10];194:952–958, <https://doi.org/10.1016/j.solener.2019.10.090>.
 15. Oleiwi HF, Rahma AJ, Salih SI, Beddai AA. Comparative study of sol-gel and green synthesis technique using orange peel extract to prepare TiO₂ nanoparticles. Baghdad Sci J. 2024 Sep 20 [cited 2025 Feb 27];21(5):1702–1711. <https://doi.org/10.21123/bsj.2023.8089>.
 16. Sofyan N, Rilda Y, Andriayani A, Angellinnov F, M'rad M, Muhammad M, *et al.* Sustainable synthesis of TiO₂ nanoparticles from gambier leaf extract for enhanced DSSC photocurrent response, Results Mater. 2025 Sept 01 [cited 2025 Nov 17];27:100752. <https://doi.org/10.1016/j.rinma.2025.100752>.
 17. Jaffri JM, Mohamed S, Ahmad IN, Mustapha NM, Manap YA, Rohimi N. Effects of catechin-rich oil palm leaf extract on normal and hypertensive rats' kidney and liver. Food Chem. 2011 Sep 15 [cited 2024 Oct 25];128(2):433–441. <https://doi.org/10.1016/j.foodchem.2011.03.050>.
 18. Tan R, Mohamed S, Samaneh GF, Noordin MM, Goh YM, Manap MYA. Polyphenol rich oil palm leaves extract reduce hyperglycaemia and lipid oxidation in STZ-rats. Int Food Res J. 2011 Jan 20;18:179–188.
 19. Azim MFF, Nisa KK, Hayati S, Apriliani NL, Afandi AD, As-tuti W. Effervescent formulation of oil palm leaf extract as a free radical scavenger. In E3S Web of Conferences. 2024 Oct 03 [cited 2025 Feb 26];576:06016. <https://doi.org/10.1051/e3sconf/202457606016>.
 20. Harmileni H, Hidayani TR, Chiuman L, Marfitania T. Antibacterial activity of palm leaf extract against Propionibacterium acnes and Staphylococcus aureus. J Prima Medika Sains. 2024 June 27 [cited 2025 Feb 26];6(1):1–5. <https://doi.org/10.34012/jpms.v6i1.5258>.
 21. Setiabudi HD, Jusoh R, Suhaimi SFRM, Masrur SF. Adsorption of methylene blue onto oil palm (Elaeis guineensis) leaves: Process optimization, isotherm, kinetics and thermodynamic studies. J Taiwan Inst Chem Eng. 2016 June 01 [cited 2025 Feb 26];63:363–370. <https://doi.org/10.1016/j.jtice.2016.03.035>.
 22. Febriani A, Syafriana V, Afriyando H, Djuhariah YS. The utilization of oil palm leaves (Elaeis guineensis Jacq.) waste as an antibacterial solid bar soap. IOP Conference Series: Earth Environ Sci. 2020 Oct 07 [cited 2025 Feb 26];572. <https://doi.org/10.1088/1755-1315/572/1/012038>.
 23. Almeida L A, Dosen A, Viol J, Marinkovic B A, TiO₂-acetylacetone as an efficient source of superoxide radicals under reduced power visible light: Photocatalytic degradation of chlorophenol and tetracycline. Catalysts. 2022 Feb 1 [cited 2025 May 11];12(2):116. <https://doi.org/10.3390/catal12020116>.
 24. Maurya IC, Singh S, Senapati S, Srivastava P, Bahadur L. Green synthesis of TiO₂ nanoparticles using Bixa orellana seed extract and its application for solar cells. Solar Energy. 2019 Dec 01 [cited 2024 Oct 25];194:952–958. <https://doi.org/10.1016/j.solener.2019.10.090>.
 25. Gu T, Tan B, Liu J, Chen J, Wei H, Zhang F, *et al.* Insight into the corrosion inhibition performance of Jasmine flower extract on copper in sulfuric acid medium using experimental and theoretical calculation methods. J Taiwan Inst Chem Eng. 2023 Sep 01 [cited 2025 Feb 26];150. <https://doi.org/10.1016/j.jtice.2023.105047>.
 26. Dias MC, Pinto DCGA, Silva AMS. Plant flavonoids: Chemical characteristics and biological activity. Molecules. 2021 Sep 01 [cited 2025 Feb 26];26(17):5377 <https://doi.org/10.3390/molecules26175377>.
 27. Roy J. The synthesis and applications of TiO₂ nanoparticles derived from phytochemical sources. J Ind Eng Chem. 2022 Feb 25 [cited 2025 Feb 26];106:1–19. <https://doi.org/10.1016/j.jiec.2021.10.024>.
 28. Einkauf JD, Bryantsev VS, Custelcean R. Anti-electrostatic hydrogen-bonded tellurate dimers captured and stabilized by crystallization of a bis-iminoguanidinium salt. Polyhedron. 2022 Sep 01 [cited 2025 Feb 26];223. <https://doi.org/10.1016/j.poly.2022.115990>.
 29. Sun C, Liu LM, Selloni A, Lu GQ, Smith SC. Titania-water interactions: A review of theoretical studies. J Mater Chem. 2010 Dec 14 [cited 2025 Feb 26];20(46):10319–10334. <https://doi.org/10.1039/c0jm01491e>.
 30. Aravind M, Amalanathan M, Mary MSM. Synthesis of TiO₂ nanoparticles by chemical and green synthesis methods and their multifaceted properties. SN Appl Sci. 2021 Apr 1 [cited 2025 May 15];3(4). <https://doi.org/10.1007/s42452-021-04281-5>.
 31. Sagadevan S, Imteyaz S, Murugan B, Lett JA, Sridewi N, Weldegebriela GK, *et al.* A comprehensive review on green synthesis of titanium dioxide nanoparticles and their diverse biomedical applications. Green Proc Syn. 2022 Jan 1 [cited 2025 May 15];11(1):44–63. <https://doi.org/10.1515/gps-2022-0005>.
 32. Makuła P, Pacia M, Macyk W. How to correctly determine the band gap energy of modified semiconductor photocatalysts based on UV-vis spectra. J Phys Chem Lett. 2018 Dec 06 [cited 2025 Feb 24];9(23):6814–6817. <https://doi.org/10.1021/acs.jpcllett.8b02892>.
 33. Nagaraj G, Raj AD, Irudayaraj AA, Josephine RL. Tuning the optical band gap of pure TiO₂ via photon induced method. Optik (Stuttg). 2019 Feb 01 [cited 2025 Feb 24];179:889–894. <https://doi.org/10.1016/j.ijleo.2018.11.009>.
 34. Kumar P, Vahidzadeh E, Thakur UK, Kar P, Alam KM, Goswami A, *et al.* C3N5: A low bandgap semiconductor containing an azo-linked carbon nitride framework for photocatalytic, photovoltaic and adsorbent applications. J Am Chem Soc. 2019 April 3 [cited 2025 May 11];141(13):5415–5436. <https://doi.org/10.1021/jacs.9b00144>.
 35. Ying S, Guan Z, Ofogebu PC, Clubb P, Rico C, He F, *et al.* Green synthesis of nanoparticles: Current developments and limitations. Environ Technol Innov. 2022 May 01 [cited 2025 Feb 26];26. <https://doi.org/10.1016/j.eti.2022.102336>.
 36. Nabi G, Majid A, Riaz A, Alharbi T, Arshad Kamran M, Al-Habardi M. Green synthesis of spherical TiO₂ nanoparticles using Citrus Limetta extract: Excellent photocatalytic water decontamination agent for RhB dye. Inorg Chem Commun. 2021 July 01 [cited 2025 Feb 26];129. <https://doi.org/10.1016/j.inoche.2021.108618>.
 37. Stokroos I, Kalicharan D, Van Der Want JLL, Jongbloed WL. A comparative study of thin coatings of Au/Pd, Pt and Cr produced by magnetron sputtering for FE-SEM. J Microsc.

- 1998 Aug 11;189:79–89. <https://doi.org/10.1046/j.1365-2818.1998.00282.x>.
38. Li MY, Sui M, Pandey P, Zhang QZ, Kunwar S, Salamo GJ, *et al*. Precise control of configuration, size and density of self-assembled Au nanostructures on 4H-SiC (0001) by systematic variation of deposition amount, annealing temperature and duration. *CrystEngComm*. 2016 May 21 [cited 2025 Feb 26]; 18(19):3347–3357. <https://doi.org/10.1039/c5ce02439k>.
39. Dubey RS, Krishnamurthy KV, Singh S. Experimental studies of TiO₂ nanoparticles synthesized by sol-gel and solvothermal routes for DSSCs application. *Results Phys*. 2019 Sep 01 [cited 2025 Feb 26];14. <https://doi.org/10.1016/j.rinp.2019.102390>.
40. Baby R, Nixon PD, Kumar NM, Subathra MSP, Ananthi N. A comprehensive review of dye-sensitized solar cell optimal fabrication conditions, natural dye selection, and application-based future perspectives. *Environ Sci Pollut Res*. 2022 Jan 01 [cited 2025 Feb 26];29(1):371–404. <https://doi.org/10.1007/s11356-021-16976-8>.
41. Devesa S, Rooney AP, Graça MP, Cooper D, Costa LC. Williamson-hall analysis in estimation of crystallite size and lattice strain in Bi_{1.34}Fe_{0.66}Nb_{1.34}O_{6.35} prepared by the sol-gel method. *Mater Sci Eng: B*. 2021 Jan 01 [cited 2025 Feb 26];263. <https://doi.org/10.1016/j.mseb.2020.114830>.
42. Triviño-Bolaños DF, Camargo-Amado RJ. Synthesis and characterization of porous structures of rutile TiO₂ /Na_{0.8}Ti₄O₈/Na₂Ti₆O₁₃ for biomedical applications. *MethodsX*. 2019 Jan 01 [cited 2025 Feb 26];6:1114–1123. <https://doi.org/10.1016/j.mex.2019.04.002>.
43. El Koulali F, Ouzzine M, Cano-Casanova L, Román-Martínez MC, Lillo-Ródenas MA. Use of the HighScore plus software for an easy and complete quantification of the anatase, brookite, rutile, and amorphous phase content in TiO₂. *Chem Inorg Mater*. 2025 Jan 04 [cited 2025 Feb 26];5:100086. <https://doi.org/10.1016/j.cinorg.2024.100086>.
44. Khalid A, Ahmad P, Alharthi AI, Muhammad S, Khandaker MU, Faruque MRI, *et al*. Unmodified titanium dioxide nanoparticles as a potential contrast agent in photon emission computed tomography. *Crystals*. 2021 Feb 01 [cited 2025 Feb 26];11(2):1–10. <https://doi.org/10.3390/cryst11020171>.
45. Frank O, Zukalova M, Laskova B, Kürti J, Koltai J, Kavan L. Raman spectra of titanium dioxide (anatase, rutile) with identified oxygen isotopes (16, 17, 18). *Phys Chem Chem Phys*. 2012 Nov 14 [cited 2025 Feb 26];14(42):14567–14572. <https://doi.org/10.1039/c2cp42763j>.
46. Eddy DR, Permana MD, Sakti LK, Sheha GAN, Solihudin GAN, Hidayat S, *et al*. Heterophase polymorph of TiO₂ (anatase, rutile, brookite, TiO₂ (B)) for efficient photocatalyst: fabrication and activity. *Nanomaterials*. 2023 Feb 01 [cited 2025 Feb 26];13(4). <https://doi.org/10.3390/nano13040704>.
47. Madden E, Zwijnenburg MA. The effect of particle size on the optical and electronic properties of hydrogenated silicon nanoparticles. *Phys Chem Chem Phys*. 2024 Mar 21 [cited 2025 Feb 27];26(15):11695–11707. <https://doi.org/10.1039/d4cp00119b>.
48. Qourzal S, Assabbane A, Ait-Ichou Y. Synthesis of TiO₂ via hydrolysis of titanium tetraisopropoxide and its photocatalytic activity on a suspended mixture with activated carbon in the degradation of 2-naphthol. *J Photochem Photobiol A Chem*. 2004 May 21 [cited 2025 May 12];163(3):317–321. <https://doi.org/10.1016/j.jphotochem.2003.12.013>.
49. Saini R, Kumar P. Green synthesis of TiO₂ nanoparticles using tinospora cordifolia plant extract & its potential application for photocatalysis and antibacterial activity. *Inorg Chem Commun*. 2023 Oct 1 [cited 2025 May 12];156. <https://doi.org/10.1016/j.inoche.2023.111221>.

استخلاص أوراق نخيل الزيت (*Elaeis guineensis*) كوسيط في التخليق الأخضر لجزيئات ثاني أكسيد التيتانيوم (TiO_2) وخصائصها البصرية

نوفريجون سفيان^{1,2}، أندرياني³، يتريا ريلدا⁴، فيونا أنجيلينوف²، مونا مراد⁵، محمد²، آغا ريدوفا⁶، أحمد هيرمان يونو^{1,2}، دونانتا دانيسوارا^{1,2}

¹مركز أبحاث المواد المتقدمة، كلية الهندسة، جامعة إندونيسيا، ديبوك 16424، إندونيسيا.

²قسم هندسة المعادن والمواد، كلية الهندسة، جامعة إندونيسيا، ديبوك 16424، إندونيسيا.

³قسم الكيمياء، كلية الرياضيات والعلوم الطبيعية، جامعة سومطرة أوتارا، ميدان 20155، إندونيسيا.

⁴قسم الكيمياء، كلية الرياضيات والعلوم الطبيعية، جامعة الأندلس، بادانج، 25163، إندونيسيا.

⁵قسم اللياقة البدنية، جامعة باريس ساكلاي، باتيمنت بريجيت، 91190، فرنسا.

⁶مركز أبحاث المعادن، الوكالة الوطنية للبحث والابتكار، تانجيرانج سيلاتان، بانن 15314، إندونيسيا.

الملخص

يهدف هذا العمل إلى استكشاف خصائص جزيئات ثاني أكسيد التيتانيوم النانوية (TiO_2 NPs) المصنعة بطريقة صديقة للبيئة باستخدام مستخلص أوراق نخيل الزيت (*Elaeis guineensis*) كوسط أخضر وعامل تغليف، من خلال استخدام رباعي إيزوبروبوكسيد التيتانيوم (TTIP) كمادة أولية. تم استخلاص أوراق نخيل الزيت باستخدام تركيزات مختلفة من المذيبات. وقد تم تمييز المستخلص الطبيعي باستخدام الكروماتوغرافيا السائلة مع مطياف الكتلة (LC-MS) والطيفية تحت الحمراء لاكتشاف المحتويات الكيميائية النشطة والمجموعات الوظيفية. تم أيضًا تمييز جزيئات TiO_2 النانوية المتحصل عليها باستخدام الطيفية تحت الحمراء (FTIR) للمجموعات الوظيفية، والطيفية فوق البنفسجية للخصائص البصرية (UV-DRS)، والانحراف بالأشعة السينية (XRD) لتكوين الطور والخصائص التبلورية. تم استخدام أجهزة متطورة مثل مجهر إلكترون المسح الانبعاثي الميداني المجهز بمطياف الأشعة السينية المشتت للطاقة (FESEM/EDX) وظيفية رامن للكشف عن خصائص جزيئات TiO_2 النانوية المتحصل عليها. أظهرت نتائج الانحراف بالأشعة السينية أن جزيئات TiO_2 النانوية المتحصل عليها تمتلك بنية كريستالية من نوع الأناز النقي. كما لوحظ اتجاه في انخفاض طاقة الفجوة الإلكترونية لجزيئات TiO_2 النانوية مع استخدام مستخلص أوراق نخيل الزيت كوسط أخضر. تم التأكيد على أن الوسط الأخضر يؤثر على الخصائص البصرية لجزيئات TiO_2 النانوية المصنعة من خلال تقليل طاقة الفجوة من 3.2 إلكترون فولت للعينات التجارية وتلك المصنعة باستخدام الإيثانول فقط إلى 3.12 إلكترون فولت باستخدام الوسط الأخضر من مستخلص أوراق نخيل الزيت. توفر هذه النتائج رؤى لطرق تصنيع نانوية صديقة للبيئة وأكثر ابتكارًا.

الكلمات المفتاحية: التخليق الأخضر، الجزيئات النانوية، مستخلص النبات الطبيعي، زيت النخيل، ثاني أكسيد التيتانيوم.